



Review

Anion sensing by rhenium(I) carbonyls with polarized N–H recognition motifs

Kai-Chi Chang^a, Shih-Sheng Sun^{a,*}, Alistair J. Lees^{b,*}^a Institute of Chemistry, Academia Sinica, 128 Academia Road, Section 2, Taipei 115, Taiwan, ROC^b Department of Chemistry, State University of New York at Binghamton, Binghamton, NY 13902-6016, USA

ARTICLE INFO

Article history:

Available online 9 February 2012

Dedicated to Prof. Jon Zubieta

Keywords:

Anion recognition
 Rhenium(I) carbonyls
 Hydrogen-bonding interaction
 Colorimetric sensing
 Luminescent sensing

ABSTRACT

This article describes our recent research results on several rhenium(I) carbonyls complexes with polarized N–H recognition motifs as anion receptors. Structurally simple and easily synthesized luminescent anion receptors containing an amide-type anion binding site and a rhenium(I) tricarbonyl pyridine signaling unit have been developed, and they display outstanding sensitivity and selectivity toward a variety of anionic species. Moreover, thioamides and thiourea derivatives of 2,6-pyridinedicarbonyl dichloride, isophthaloyl dichloride and terephthaloyl dichloride have been synthesized. These ligands have been incorporated in dinuclear rhenium(I) diimine tricarbonyl complexes and provide anion recognition properties in these complexes. Furthermore, the related rhenium(I) complex featuring sulfonamide interacting sites that incorporate the highly chromophoric π -conjugated quinoxaline moiety has been prepared, characterized, and its photophysical properties were also studied.

© 2012 Elsevier B.V. All rights reserved.



Kai-Chi Chang received his BS (2002) in chemistry from Tunghai University, Taiwan, a MS (2004) and a PhD (2008) in applied chemistry at National Chiao Tung University under the supervision of Professor Wen-Sheng Chung. Since then he has been a postdoctoral researcher in the group of Professor Shih-Sheng Sun at the Institute of Chemistry, Academia Sinica, Taiwan. His research interests include host-guest chemistry and supramolecular self-assembly. Currently, he is a postdoctoral fellow in Professor Chain-Shu Hsu's group working on the development of polymer solar cells.



Shih-Sheng Sun studied chemistry at National Cheng Kung University (BS 1989, MS 1991) and completed his PhD (2001) in Supramolecular Chemistry at State University of New York at Binghamton with Prof. Alistair J. Lees. After two-year postdoctoral studies at Northwestern University with Prof. Joseph T. Hupp and Prof. SonBin T. Nguyen, he joined the Institute of Chemistry, Academia Sinica as an Assistant Research Fellow in 2003 and was promoted to an Associated Research Fellow in 2009. His research interests focus on supramolecular materials chemistry and their applications in molecular recognition and sensing and optoelectronic materials.

* Corresponding authors.

E-mail address: a Lees@binghamton.edu (A.J. Lees).



Alistair J. Lees studied chemistry at the University of Newcastle-upon-Tyne and received his BSc Honors in 1976 and his PhD in 1979. His PhD studies were in the area of inorganic spectroscopy with Dr. Brian B. P. Straughan. After a two-year postdoctoral fellowship (1979–81) at the University of Southern California with Prof. Arthur W. Adamson in the area of photophysics and photochemistry of metal complexes, he joined the chemistry faculty at the State University of New York at Binghamton as an Assistant Professor in 1981. He has been a Full Professor at the University since 1989 and his research interests are in synthesis, spectroscopy and photochemistry of organometallic complexes, especially studying excited states and luminescence properties, and the photophysical processes that take place in these materials.

Contents

1. Introduction	17
2. Amide bridged rhenium(I) complexes as luminescent anion receptors	17
2.1. Preparation of amide bridged rhenium(I) complexes	17
2.2. Photophysical properties	19
2.3. Anion sensing studies	19
3. Thioamide and thiourea bridged rhenium(I) complexes as luminescent anion	22
3.1. Preparation of thioamide and thiourea bridged rhenium(I) complexes	22
3.2. Photophysical properties	23
3.3. Anion sensing studies	24
4. Quinoxalinebis(sulfonamide) bridged rhenium(I) complex as a novel anion receptor	26
4.1. Preparation of quinoxalinebis(sulfonamide) bridged rhenium(I) complex	26
4.2. Photophysical properties	26
4.3. Anion sensing studies	26
5. Concluding remarks	27
Acknowledgments	27
References	27

1. Introduction

The development of new chemosensors for anions is an important subject in the field of supramolecular chemistry due to their fundamental role in biological, environmental, and chemical processes [1]. Compared to the well-developed field of cation binding and sensing, anion recognition is a more challenging field because of the variable size, shape, and strong solvation of the species [2]. As anions are larger than their isoelectronic cations and, thus, have a smaller charge-to-radius ratio, electrostatic interactions are less effective for anions than their corresponding isoelectronic cations [3]. Solvation effects are also more prominent for anions than their isoelectronic cations, and this is an important factor to consider in designing artificial anion receptors. Hydroxylic solvents usually form strong hydrogen bonds with anions, and this will reduce the affinity of anions toward anion receptors. Hydrophobicity can also influence the selectivity of an anion receptor as hydrophobic anions tend to bind more tightly to the hydrophobic sites of the receptors. Therefore, to achieve the desired sensitive and selectivity, the combination of electrostatic attraction, hydrogen bonding, hydrophobic effects, and stacking effects all need to be taken into consideration when designing artificial anionic hosts [4].

The incorporation of luminescent chromophores into the receptor, which are sensitive to interactions between the host and guest molecules, has recently gained considerable attention due to their high sensitivity and low detection limit [5,6]. The appeal of sensors that contain luminescence chromophores stems from the high sensitivity of luminescence detection compared to other spectroscopic methods. The binding of anionic species to the recognition sites leads to changes in certain properties of the receptors (such as absorption spectra, luminescence intensity, lifetime, etc.) that then serve as an indicator of guest association.

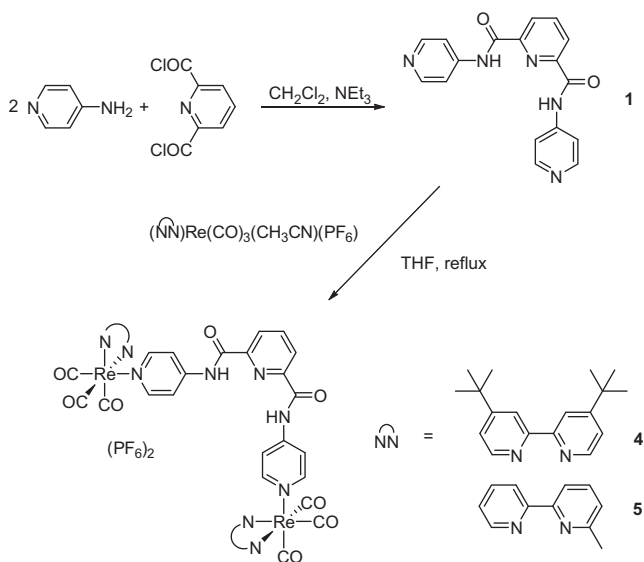
Incorporating a transition metal into the framework of sensory systems offers several advantages over pure organic sensors. Firstly, transition-metal complexes are often positively charged or electron deficient in nature. This property leads to either the enhancement of the electrostatic interactions with negatively charged species or a higher probability of orbital overlap and, thus, stronger bonding interactions with anionic species. Secondly, transition-metal complexes typically possess precisely defined geometries. This characteristic is especially useful for enhancing the selectivity of certain shaped anions or inducing unusual structural changes upon binding to anions. Thirdly, and perhaps the most appealing reason, is that transition-metal complexes possess a variety of unique functionalities such as redox activity, visible spectroscopic features (color), magnetism, luminescence, and catalytic ability. Incorporation of these functionality properties into sensory systems provides for not only the improvement of sensor technology but also some other guest recognition based applications, such as anion transport, drug delivery, and catalysis.

Herein, we review some of our recent results and focus on different types of rhenium(I) carbonyls complexes with polarized N–H recognition motifs as anion receptors: (a) new tweezer amide bridged rhenium(I) complexes [7,8]; (b) two-armed thioamide and thiourea bridged rhenium(I) complexes [9]; and (c) a novel quinoxalinebis(sulfonamide) bridged rhenium(I) complex [10].

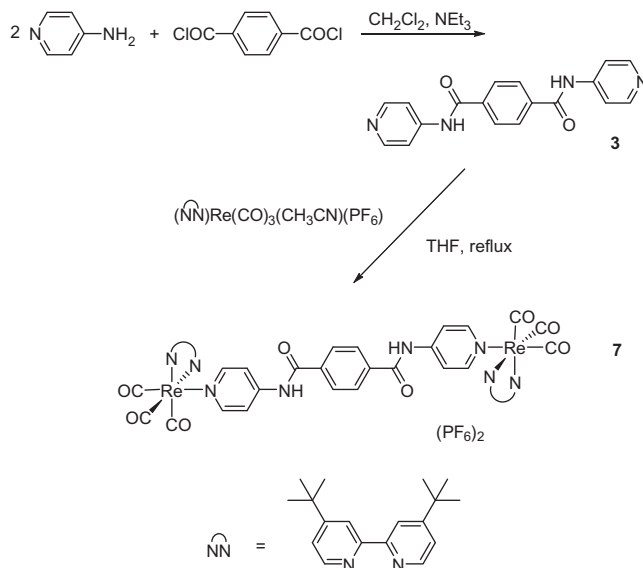
2. Amide bridged rhenium(I) complexes as luminescent anion receptors

2.1. Preparation of amide bridged rhenium(I) complexes

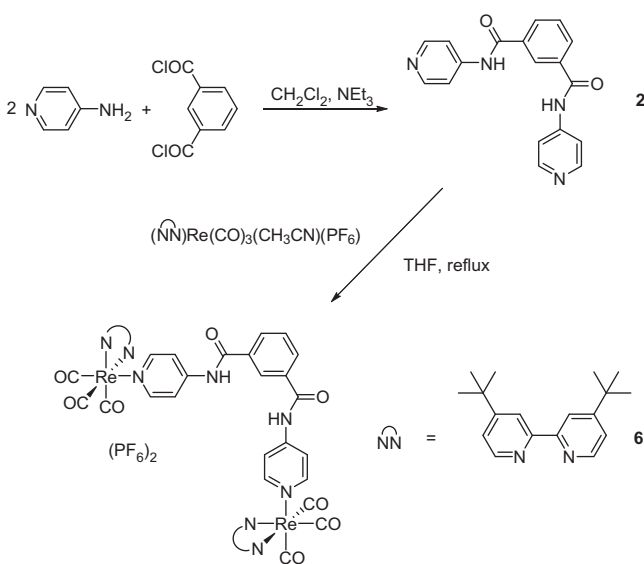
The syntheses of amide ligand **1** and complexes **4** and **5** are shown in Scheme 1. The bridging ligand **1** was prepared in 56%



Scheme 1. Synthesis of the amide ligand **1** and complexes **4** and **5**.



Scheme 3. Synthesis of the amide ligand **3** and complex **7**.



Scheme 2. Synthesis of the amide ligand **2** and complex **6**.

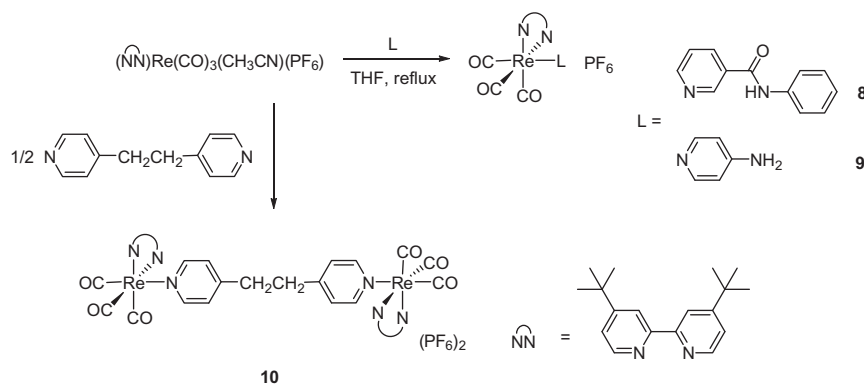
yield from 2 equiv. of 4-aminopyridine and 2,6-pyridinedicarbonyl dichloride. Ligand **1** exhibits very poor solubility in most common organic solvents, presumably because of its potential for intermolecular hydrogen-bonding formation via the amide protons. Subsequent reaction of **1** and 2 equiv. of $(\text{CH}_3\text{CN})(4,4'\text{-}t\text{Bu}_2\text{bpy})\text{Re}(\text{CO})_3(\text{PF}_6)$ or $(\text{CH}_3\text{CN})(6\text{-Mebpy})\text{Re}(\text{CO})_3(\text{PF}_6)$ in refluxing THF, followed by recrystallization from CH_2Cl_2 /pentane (**4**) or CH_3CN /ether (**5**), afforded bright yellow crystalline solids **4** and **5** in 81% and 88% yields, respectively.

The syntheses of amide ligand **2** and complex **6** are shown in Scheme 2. The bridging ligand **2** was prepared in 62% yield from 2 equiv. of 4-aminopyridine and isophthaloyl dichloride. Due to the extremely low solubility of ligand **2** in THF, the subsequent metal-complexation process needed to reflux for 3 days to ensure the completion of the reaction. The yellowish powder of complex **6** was isolated after recrystallization from CH_2Cl_2 /hexane in 82% yield.

Similarly, the syntheses of amide ligand **3** and complex **7** are shown in Scheme 3. Ligand **3** was synthesized in 62% yield from 2 equiv. of 4-aminopyridine and terephthaloyl chloride. It has been found the reaction can be carried out only with a relative small amount of starting materials and with a large quantity of solvent to ensure the solubility of the condensation products. Subsequent reaction of **3** and 2 equiv. of $(\text{CH}_3\text{CN})(4,4'\text{-}t\text{Bu}_2\text{bpy})\text{Re}(\text{CO})_3(\text{PF}_6)$ in refluxing THF, followed by recrystallization from CH_2Cl_2 /hexane, afforded a bright yellow crystalline solid **7** in 78% yield.

Complexes **8–10** were synthesized from reaction of $(\text{CH}_3\text{CN})(4,4'\text{-}t\text{Bu}_2\text{bpy})\text{Re}(\text{CO})_3(\text{PF}_6)$ and nicotinamide, 4-NH₂-py, or 0.5 equiv. of BPA in refluxing THF, as shown in Scheme 4, and purified by recrystallization from CH_2Cl_2 /hexane solution, which afforded pale yellow microcrystals in 76% yield for **8**, 92% yield for **9**, and 86% yield for **10**. The identity and purity of all new compounds have been established by NMR, mass spectrometry, and elemental analysis.

The N–H protons of complex **4** exhibit a chemical shift of 10.59 ppm in CDCl_3 . The highly downfield chemical shift in a non-hydrogen bond donating solvent indicates the presence of strong intramolecular hydrogen bonding between the N–H protons and the nitrogen of the central pyridine. This results in ligand **1** having an approximate right angle geometry [11], and the converged structure of complex **4** renders it as an effective anion receptor through hydrogen bonding. Similarly, the highly downfield chemical shift (11.06 ppm) of the amide protons is also observed in complex **5**. It should be pointed out, however, that the more downfield shifting of the amide protons in complex **5** compared to those in complex **4** could be simply due to the presence of trace amounts of water in the deuterated acetone, not really indicating a stronger hydrogen bonding in complex **5** than in complex **4**. In the case of complex **8**, the *meta* connection between the amide group and nitrogen in the pyridine results in no intramolecular hydrogen bonding, and it is obvious that the chemical shift of the amide proton appears at the normal position, ca. 8.34 ppm. In the cases of complexes **6** and **7**, there is no chance to form intramolecular hydrogen bonding, but there may be intermolecular hydrogen bonding between the amide protons and the carbonyl groups. This idea is tentatively supported by the slightly downfield shifting of the amide protons at 8.96 and 9.10 ppm for complexes **6** and **7**, respectively. Complexes **9** and **10** were also synthesized to serve as model compounds. Complex **10** is employed to assess



Scheme 4. Synthesis of the complexes 8–10.

Table 1

Absorption and emission spectral data and calculated photophysical parameters of complexes 4–10 in CH₂Cl₂ at 293 K.

Complexes	Absorption	Emission				
	λ_{max} , nm ($10^{-3}\epsilon$, M ⁻¹ cm ⁻¹)	λ_{em} , nm	Φ_{em}	τ , μs	$10^{-5}k_{\text{r}}$, s ⁻¹	$10^{-6}k_{\text{nr}}$, s ⁻¹
4	254 (63.6), 281(61.5), 380 (sh, 7.70)	536	0.20	0.48	4.2	1.7
5	252 (45.6), 300 (47.6), 324 (sh, 35.9), 368 (6.02)	544	0.083	0.38	2.2	2.4
6	255 (50.1), 285 (53.0), 315 (sh, 33.6), 362 (7.84)	538	0.16	0.62	2.6	1.3
7	255 (52.7), 288 (56.4), 303 (sh 54.5), 376 (sh, 8.03)	538	0.22	0.54	4.1	1.4
8	250 (35.2), 274 (34.7), 300 (sh, 25.6), 315 (22.1), 373 (sh, 5.11)	524	0.39	1.10	3.5	0.56
9	270 (30.6), 316 (sh, 9.82), 368 (4.09)	552	0.042	0.21	2.0	4.6
10	254 (40.9), 271 (41.6), 303 (sh, 28.1), 315 (24.8), 348 (sh, 9.42)	532	0.27	0.59	4.6	1.2

the position of MLCT band, while complex **9** is expected to form the weakest hydrogen bonding, if there is any, among all six complexes (**4–9**) studied in this paper.

2.2. Photophysical properties

The absorption and emission spectral data, including lifetimes and emission quantum yields, in deoxygenated CH₂Cl₂ at 293 K are summarized in Table 1. In general, the absorption spectra of all the complexes exhibit a series of strong absorption bands below 335 nm. These bands are assigned to ligand-based π - π^* transitions. The absorption spectra of complexes **4** and **10**, as well as their difference spectrum, are displayed in Fig. 1. The low-energy shoulder around 380 nm in complex **4** disappears in the difference spectrum, and this confirms that the lowest excited state is a Re ($d\pi$) to 4,4'-*t*Bu₂bpy (π^*) charge-transfer band. The low-energy features around 370 nm in complexes **6–8** are also assigned to Re ($d\pi$) to 4,4'-*t*Bu₂bpy (π^*) charge-transfer bands. This assignment is supported by the appearance of an absorption band at 368 nm in complex **9**, where the only low-energy transition is the Re ($d\pi$) to 4,4'-*t*Bu₂bpy (π^*) charge-transfer band. Similarly, the shoulder at 368 nm in complex **5** is assigned to a Re ($d\pi$) to 6-Mebpy (π^*) charge-transfer band.

All six complexes exhibit fairly strong luminescence in CH₂Cl₂ solution at room temperature. The structureless spectral profiles and submicrosecond lifetimes indicate that the emissions of all six complexes originate from the ³MLCT excited states. The calculated k_{r} values are also very typical for triplet MLCT emissions, ca. 1×10^5 s⁻¹ [12]. The photophysical parameters of complexes **4**, **6**, and **7** are virtually the same. This is not unexpected given that the lowest excited states in both these complexes are Re ($d\pi$) to 4,4'-*t*Bu₂bpy (π^*) CT states and the bridging ligands are structurally similar amide-pyridines.

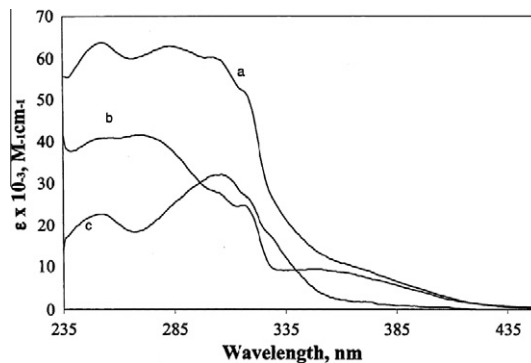


Fig. 1. Absorption spectra of complexes **4** (curve a), **10** (curve b), and the difference spectrum between complexes **4** and **10** (curve c) in CH₂Cl₂ at 293 K.

2.3. Anion sensing studies

The anionic sensory system studied here comprises an amide-pyridine moiety, which provides the anion binding site through amide-anion hydrogen bonding and a signaling unit which is (4,4'-*t*Bu₂bpy)Re(CO)₃. The positive-charged character of the (4,4'-*t*Bu₂bpy)Re(CO)₃ moiety is also expected to provide an additional electron-withdrawing effect on the amide binding site [13]. Addition of different halides or inorganic polyatomic anions (as tetrabutylammonium salts) into 2×10^{-6} M solutions of complexes **4–9** was observed to cause different degrees of quenching of the luminescence intensities. Except for complex **9**, the N–H protons in ¹H NMR spectra all showed significant downfield shifts (>1.5 ppm), indicating the strong hydrogen-bonding formation between the amide protons of the complexes and the anions. In the case of complex **9**, there is no significant decrease in the emission

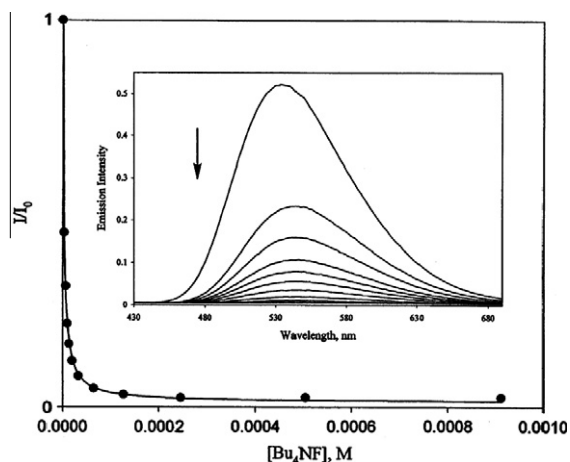


Fig. 2. Titration curve of the addition of F^- anion (as tetrabutylammonium salt) to complex **4** in CH_2Cl_2 solution as monitored by luminescence spectroscopy. The inset showed the changes to the emission spectrum of complex **4** in CH_2Cl_2 solution upon addition of F^- anion. Emission spectra of the two highest anion concentrations were not included for clarity. The excitation wavelength is 360 nm.

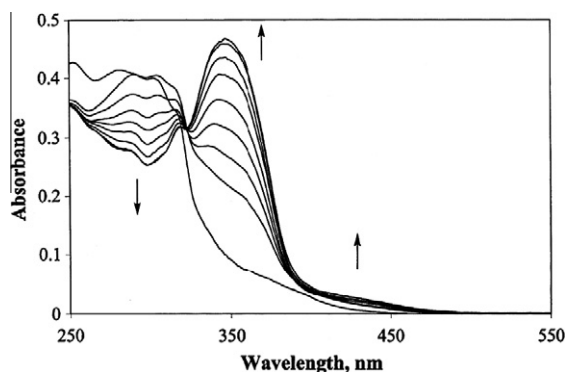


Fig. 3. Changes in the absorption spectra of complex **4** (6.7×10^{-6} M) in CH_2Cl_2 solution upon addition of F^- anion (as tetrabutylammonium salt). The concentrations of F^- anion are 0 , 4.0×10^{-5} , 5.9×10^{-5} , 9.8×10^{-5} , 1.9×10^{-4} , 3.7×10^{-4} , 6.9×10^{-4} , 1.3×10^{-3} , and 2.2×10^{-3} M, respectively.

intensity when the complex is exposed to anions. The titration curves were observed to fit well to a 1:1 binding isotherm, and the binding stoichiometry was further confirmed by Job plots [14].

Fig. 2 shows a typical 1:1 titration curve for the luminescence intensity upon addition of F^- to a CH_2Cl_2 solution of complex **4**. Concomitant with the quenching, the luminescence maximum red shifts approximately 6–10 nm in each case. The lowest-energy band (1MLCT) in the absorption spectrum also red shifts 10–30 nm in each case along with the decrease of the $\pi-\pi^*$ band at 281 nm, and a new band developed around 347 nm with a shoulder around

436 nm upon addition of anion into the receptor solution (see Fig. 3).

However, in the case of I^- , there were no apparent changes in the absorption spectrum. The red shift of the absorption and emission positions, as well as the quenching of the emission intensities upon addition of anions, are not apparent, but this is likely due to a switching of the lowest excited state from a 4,4'-*t*Bu₂bpy-based 3MLCT state to an amide-pyridine-based 3MLCT state through hydrogen-bonding formation, thereby enhancing nonradiative decay. This conclusion is partially supported by low-level extended Hückel calculations, where the LUMO changes from π^* orbital localized on 4,4'-*t*Bu₂bpy to the π^* orbital localized on the amide-pyridine ligand upon formation of hydrogen bonding between the anion and amide protons. Scheme 5 depicts possible qualitative excited-state diagrams representing the respective charge-transfer energy levels before and after anion binding. Similar red shifts on the emission spectra and quenching of the emission intensities upon anion binding were also observed in Ru(II)-polypyridine-based sensing systems [6b,15]. It appears that a dynamic quenching mechanism does not occur in this system, given the fact that there was no apparent quenching between complex **10** and the various anions studied. Another possible explanation for the observed emission quenching behavior is anion-enhanced reductive quenching of the $MLCT$ excited state; this would also be expected to lower the energy of the Re(I) to pyridine-amide ligand charge-transfer excited state.

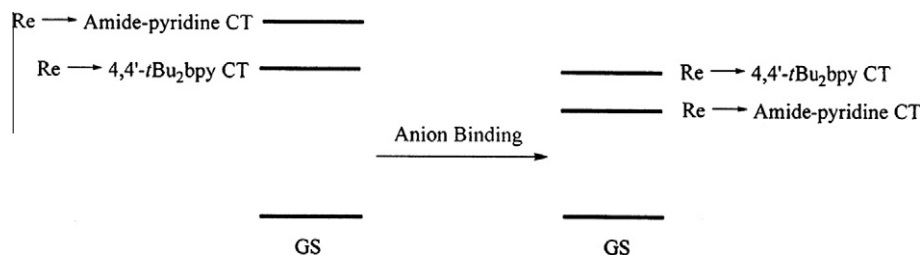
Table 2 summarizes the binding constants measured for complexes **4–8** toward different anions. Clearly, complexes **4** and **5** show strong binding affinity toward halides, cyanide, or acetate anions, only moderate binding affinity toward dihydrogen phosphate, and very weak binding affinity to nitrate or perchlorate anions. The overall order determined for binding affinity is the following: $CN^- > F^- > I^- > Cl^- \sim Br^- \sim OAc^- \gg H_2PO_4^- > NO_3^- > ClO_4^-$. This finding is significant as it is unusual for charged receptors to exhibit such outstanding selectivity for anion species

Table 2

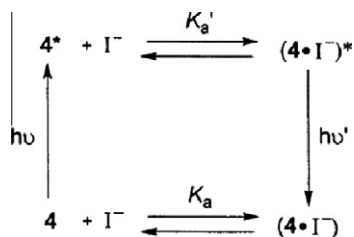
Association constants K_a of complexes **4–8** toward different anions determined by luminescence titration in CH_2Cl_2 at 298 K.

Anions	$10^{-3}K_a, M^{-1}$				
	4	5	6	7	8
CN^-	88	14	1.5	2.3	1.5
F^-	38	2.8	2.5	6.0	1.1
Cl^-	4.0	1.6	0.41	0.75	0.33
Br^-	3.9	2.4	0.38	0.44	0.22
I^-	15 ^a	2.7 ^a	5.7 ^a	1.1 ^a	1.6 ^a
OAc^-	3.4	1.4	0.71	0.73	1.6
$H_2PO_4^-$	0.015	0.010	18	5.5	1.6
NO_3^-	6.3×10^{-3}	5.9×10^{-3}	0.47	0.52	0.34
ClO_4^-	8.4×10^{-4}	7.4×10^{-4}	4.5×10^{-3}	2.0×10^{-3}	3.1×10^{-3}

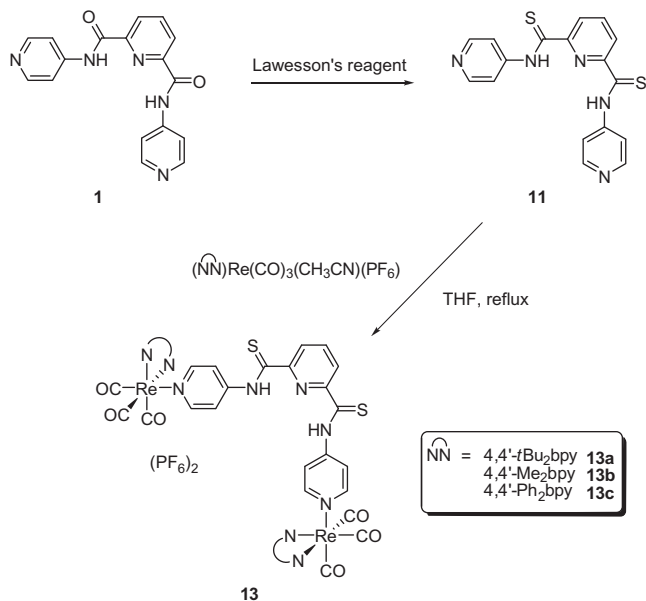
^a Possibly involves an excited-state association process. See text for details.



Scheme 5. Qualitative excited-state diagrams for charge-transfer energy levels before and after anion binding.

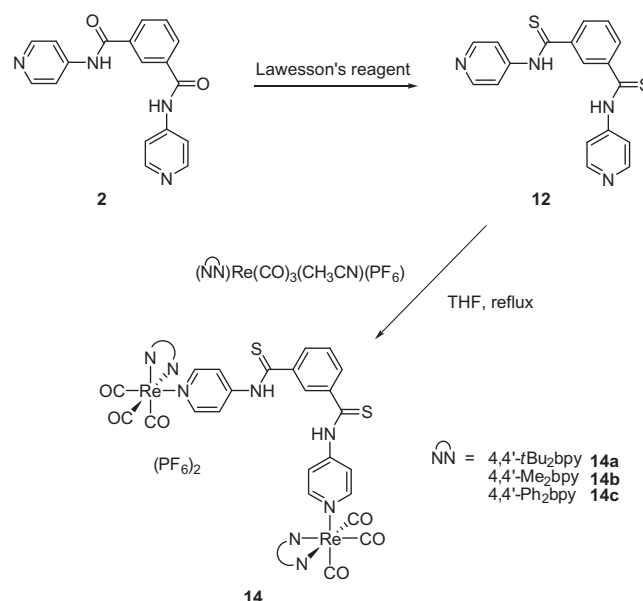


Scheme 6. An excited-state association mechanism for iodide-induced emission quenching.



Scheme 7. Synthesis of the thioamide ligand **11** and complexes **13a–13c**.

[11,16]. In fact, the combination of interactions involving electrostatic forces, hydrogen-bonding strength, hydration energy, and steric effects all apparently influence the binding affinities toward anions in complexes **4** and **5**. Importantly, the sensitivities of complexes **4** and **5** are so high that the emission intensity can be

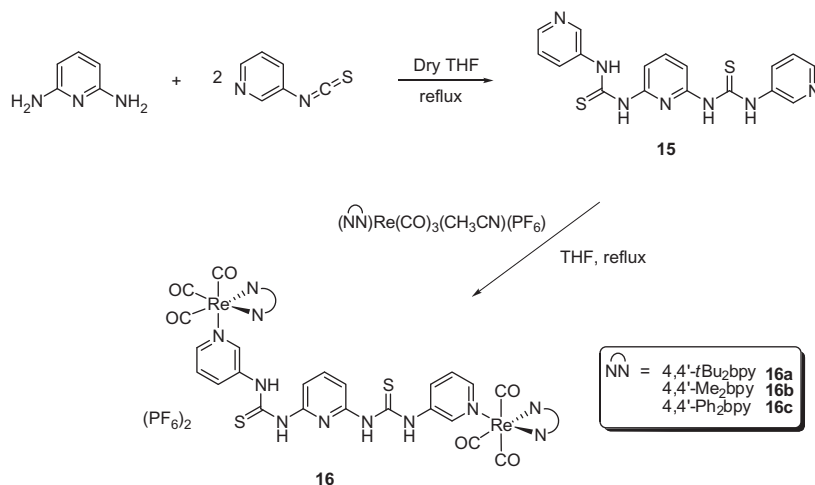


Scheme 8. Synthesis of the thioamide ligand **12** and complexes **14a–14c**.

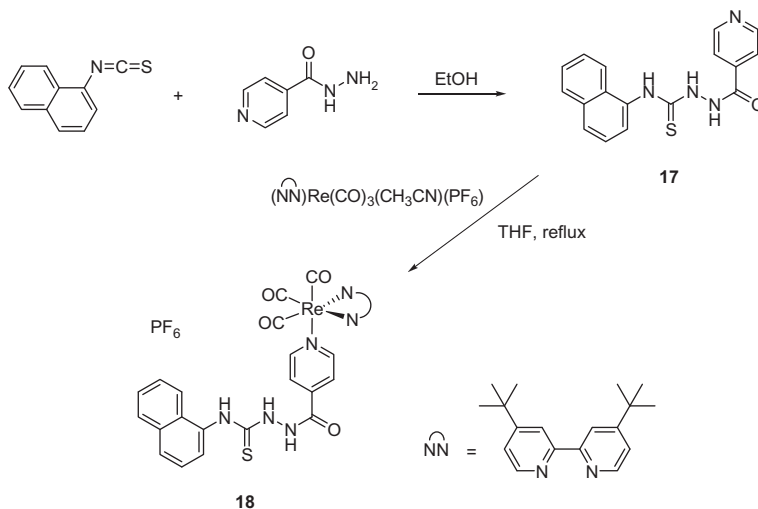
effectively quenched by as much as 10%, even in the presence of only 10^{-8} M cyanide or fluoride anions.

It is surprising that I^- has higher association constant than both the Cl^- and Br^- anions. Given the fact that there was no apparent change in the absorption spectrum upon addition of I^- to the receptor solution (vide infra), the efficient emission quenching is likely due to the involvement of an excited-state association process (see **Scheme 6**).

To account for the unusual selectivity observed in complexes **4** and **5**, several structurally similar complexes were also synthesized and their anion binding studies were conducted under the same experimental conditions. Although the general trend of sensitivity still holds in complexes **6–8**, the selectivity toward different anions is greatly reduced. Except for ClO_4^- , which is expected to form the weakest hydrogen bond, all other anions studied in this research exhibit similar binding affinities within two orders of magnitude. The similar association constants of complexes **6** and **7** toward anions indicate that the two amide groups in complex **6** are arranged in an anti-fashion. The intramolecular hydrogen-bonding capability of ligand **1**, which forces a cleft conformation, seems to be the



Scheme 9. Synthesis of the thiourea ligand **15** and complexes **16a–16c**.



Scheme 10. Synthesis of the amidothiourea ligand **17** and complex **18**.

key to its metal complexes being efficient as an anionic sensory system.

3. Thioamide and thiourea bridged rhenium(I) complexes as luminescent anion

3.1. Preparation of thioamide and thiourea bridged rhenium(I) complexes

The syntheses of thioamide ligands **11–12** and complexes **13(a–c)** and **14(a–c)** are shown in Schemes 7 and 8. The thioamide ligands **11** and **12** were prepared from 2 equiv. of Lawesson's reagent and amide ligands **1** and **2**, respectively. The resulting products were characterized by IR spectroscopy to compare with the amide and thioamide ligands. The disappearance of the C=O stretching bands at about 1600 cm^{-1} and the two bands associated with amide, due to intermolecular hydrogen bonding, served as indicators of complete thionation. It is worth noting that the synthesis of complexes **13(a–c)** and **14(a–c)** was achieved by refluxing 2 equiv. of the respective acetonitrile bipyridine rhenium(I) complexes $\{(bpy)Re(CO)_3(CH_3CN)(PF_6)\}$ with the corresponding one equivalent of the appropriate bridging ligand for 2 h. 1H NMR spectra were monitored throughout the reaction to determine

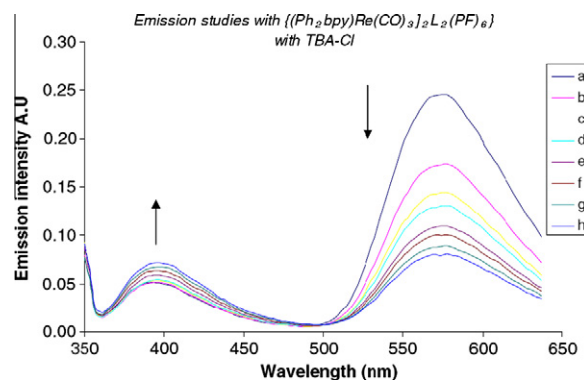


Fig. 5. Emission titration spectra of complex **16c** ($1.6 \times 10^{-5}\text{ M}$) in CH_2Cl_2 at 298 K with increasing concentrations of TBA-Cl: (a) the initial spectrum without added anion, (b) 1, (c) 2, (d) 3, (e) 4, (f) 5, (g) 6, and (h) 7 equiv. Excitation wavelength is 330 nm.

the extent of product formation. The disappearance of the peak at 2.3 ppm, which is attributed to the bound acetonitrile ligands, served as an indicator of successful ligand and coordination of the bridging ligand to the metal center.

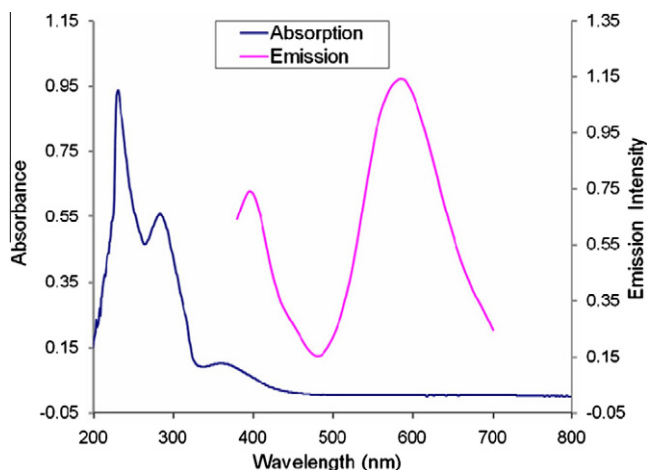


Fig. 4. Absorption spectrum (blue) and emission spectrum (pink) of $5.0 \times 10^{-6}\text{ M}$ of complex **13a** in CH_2Cl_2 at 298 K. Excitation wavelength is 360 nm.

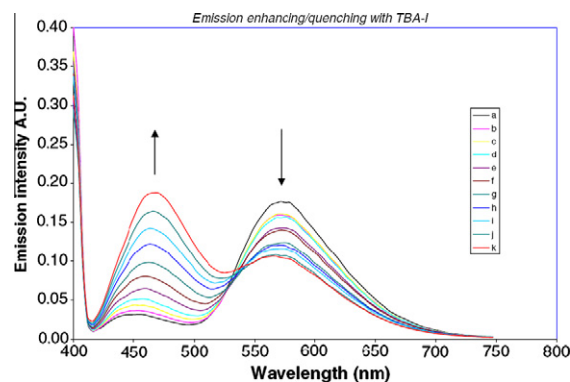


Fig. 6. Emission titration spectra of complex **16c** ($1.0 \times 10^{-5}\text{ M}$) in CH_2Cl_2 at 298 K with increasing concentrations of TBA-I: (a) the initial spectrum without added anion, (b) 0.5, (c) 1.0, (d) 2.0, (e) 2.5, (f) 3.0, (g) 3.5, (h) 4.0, (i) 4.5, (j) 5.0, and (k) 5.5 equiv. Excitation wavelength is 385 nm.

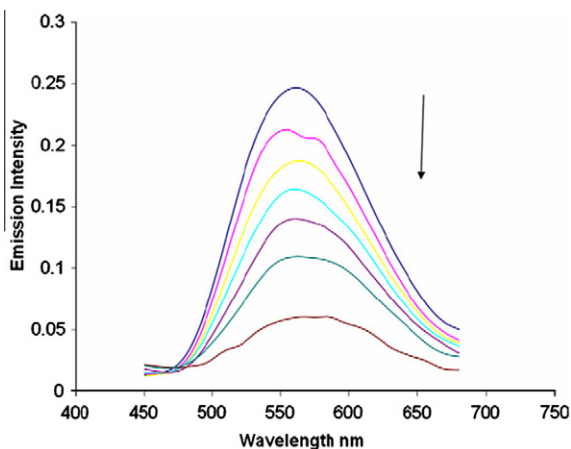


Fig. 7. Emission titration spectra of complex **13a** (2.0×10^{-5} M) in CH_2Cl_2 at 298 K adding Cl^- anion up to 6 equiv. Excitation wavelength is 360 nm.

The syntheses of thiourea ligand **15** and complexes **16(a–c)** are shown in Scheme 9. The bridging ligand **15** was synthesized in 40% yield from 2,6-diamionpyridine and 2 equiv. of 3-pyridineisothiocyanate. Subsequent reaction of **15** and 2 equiv. of the respective acetonitrile bipyridine rhenium(I) complex, $\{(\text{bpy})\text{Re}(\text{CO})_3(\text{CH}_3\text{CN})\}$

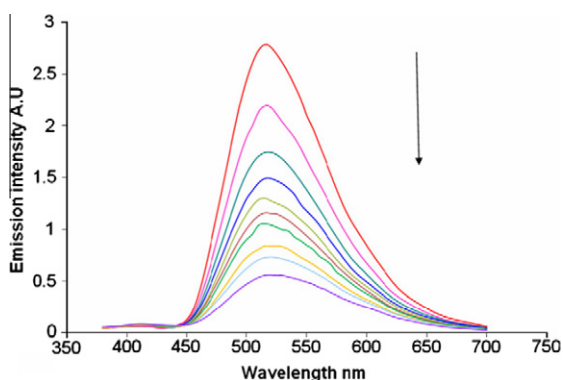


Fig. 8. Emission titration spectra of complex **13a** (2.0×10^{-5} M) in CH_2Cl_2 at 298 K adding Br^- anion in increments of 1 up to 9 equiv., with the initial spectrum having no added anion. Excitation wavelength is 360 nm.

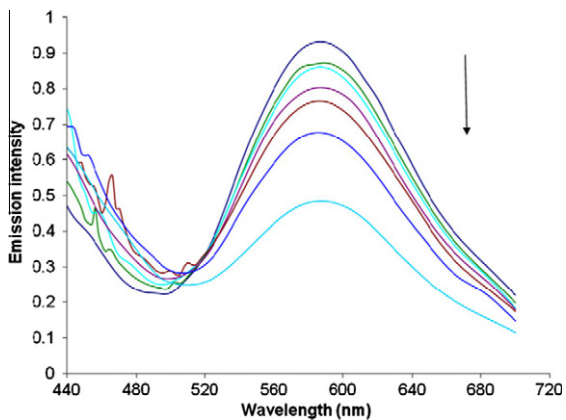


Fig. 9. Emission titration spectra of complex **13b** (5.0×10^{-6} M) in CH_2Cl_2 at 298 K with TBA-Br: adding in increments of 0.2, 0.4, 0.6, 0.8, 1.0, and 2.0 equiv. The initial spectrum has no added anion. Excitation wavelength is 360 nm.

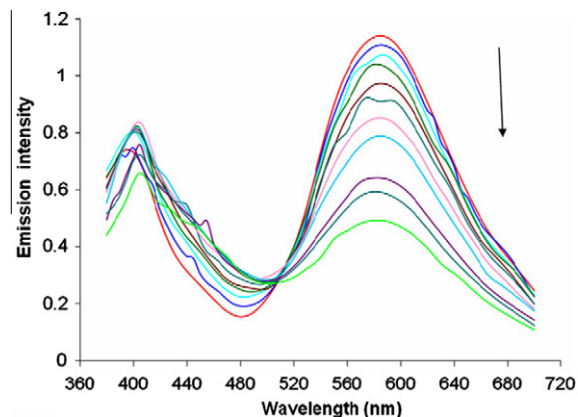


Fig. 10. Emission titration spectra of **13b** (5.0×10^{-6} M) in CH_2Cl_2 at 298 K with TBA- H_2PO_4 , in increments of 0.2, 0.4, 0.6, 0.8, 1.0, 1.2, 1.4, 1.6, 1.8, and 2.0 equiv. The initial spectrum has no added anion. Excitation wavelength is 360 nm.

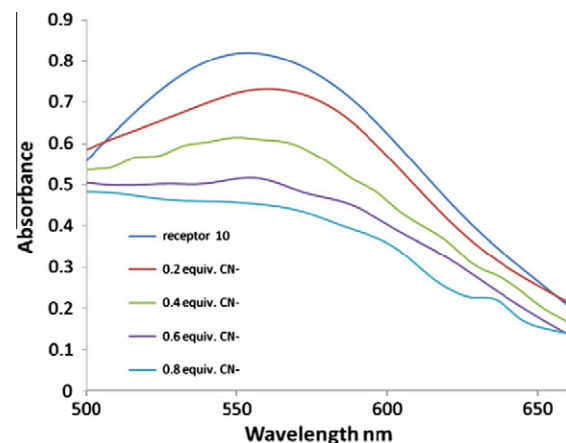


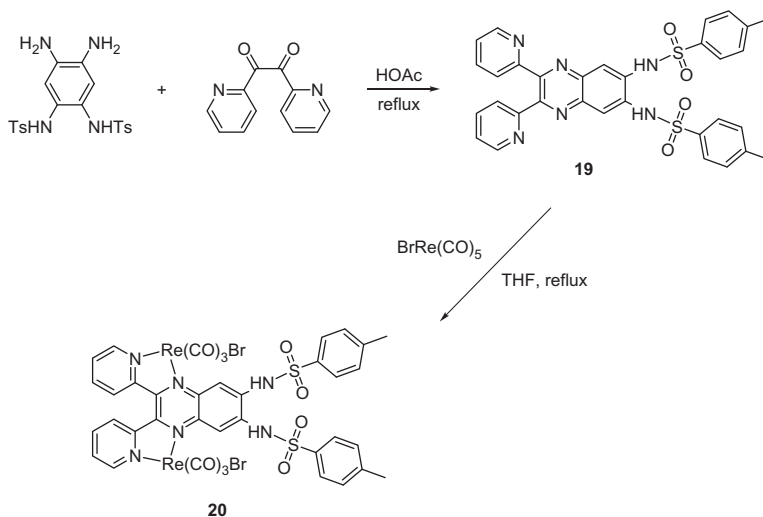
Fig. 11. Emission titration of compound **18** (1.6×10^{-5} M) in 95% $\text{H}_2\text{O}/\text{DMSO}$ (v/v) at 298 K with TBA-CN (0.2, 0.4, 0.6, and 0.8 equiv.). The initial spectrum has no added anion. Excitation wavelength is 360 nm.

(PF_6), in refluxing THF, followed by recrystallization from CH_2Cl_2 /pentane, afforded yellowish orange crystals **16(a–c)**.

The syntheses of the amidothiurea ligand **17** and the corresponding complex **18** are shown in Scheme 10. Ligand **17** was synthesized in 97% yield from isoniazid and 1-isothiocyanatonaphthalene in ethanol. Subsequent reaction of **17** and (CH_3CN) $(4,4'\text{-tBu}_2\text{bpy})\text{Re}(\text{CO})_3(\text{PF}_6)$ in refluxing THF afforded the amidothiurea-based rhenium complex **18**.

3.2. Photophysical properties

It was observed that these dinuclear rhenium complexes of the type **13a–c**, **14a–c** and **16a–c**, are yellow compounds with considerable absorption in the range 300–400 nm and only slight variations depending on the pyridyl ligand attached to the rhenium metal. Also noted was their strong emission centered at about 600 nm. Fig. 4 shows typical absorption and emission spectra of a representative complex **13a**. Both the absorption and emission spectra are dominated by higher lying intraligand (IL) and lowest energy lying metal-to-ligand charge transfer (MLCT) transitions [7].



Scheme 11. Synthesis of the sulfonamide ligand **19** and complex **20**.

Table 3
Photophysical properties of probes **19** and **20** in CH_3CN at 293 K.

Probe	Absorption	Emission			
	λ_{max} , nm ($10^{-3}\epsilon$, $\text{M}^{-1}\text{cm}^{-1}$)	λ_{em} , nm	Φ_{em}	τ , ns	
19	261 (37.5), 355 (13.2), 415 (0.6)	530	0.05	1.2	
20	324 (19.3), 439 (11.4), 550 (sh, 5.7)	604	2.6×10^{-5}	<0.1 ^a	

^a The excited-state lifetime is too short to be precisely measured in our instrument.

3.3. Anion sensing studies

The thiourea-bridged dinuclear complex **16c**, exhibited a maximum absorption at 330 nm. Upon irradiation of this compound with 330 nm light, two emission bands were observed, centered at 400 and 575 nm, respectively. Titration of complex **16c** with tetrabutylammonium chloride (see Fig. 5) resulted in emission enhancement of the higher energy band (at 400 nm) with a corresponding quenching of the lower energy band at 575 nm, and an isoemissive point at about 495–500 nm. Similar experiments were also carried out with TBA-I (tetrabutylammonium iodide) and again an enhancement of the upper energy band and a concomitant quenching of the lower energy band was observed (see Fig. 6).

The thiourea-based rhenium(I) complex **16c** was found to emit strongly at 575 nm and weakly at 465 nm upon excitation at 385 nm. Emission titration studies were carried out with TBA-I in

CH_2Cl_2 at 298 K, while exciting at 385 nm. The intensities of the two emission peaks changed with increasing addition of the iodide anion, added in the form of TBA-I. The relatively strong emission peak at 575 nm showed quenching, while the initially less emissive band at 465 nm exhibited significant enhancement resulting in the formation of an isoemissive point at 530 nm (see Fig. 6). The association constant for **16c** with TBA-I in CH_2Cl_2 was calculated to be $2.96 \times 10^4 \text{ M}^{-1}$ by a Stern–Volmer plot.

Emission titration studies of the complex **13a** were carried out in CH_2Cl_2 , where the addition of tetrabutylammonium chloride resulted in the emission quenching of the band at about 560 nm following excitation at 352 nm (see Fig. 7). A similar quenching pattern was observed for the other anions such as fluoride and bromide, with fluoride showing the most significant response in this category.

In order to study the interactions of anions with this receptor, UV–Vis spectrophotometric titrations in dichloromethane were carried out. It should be noted that dichloromethane was chosen because it is relatively nonpolar, aprotic and does not interfere with the receptor–anion hydrogen bonding. These results did not differ much from the amide counterparts reported earlier [7]. However it should be pointed out that the solubility of these new thiourea, urea and thiourea ligands in organic solvents was relatively better than their amide counterparts.

The emission titration shown in Fig. 8 indicates how the addition of bromide to complex **13a** with the triflate (OTf^-) counter

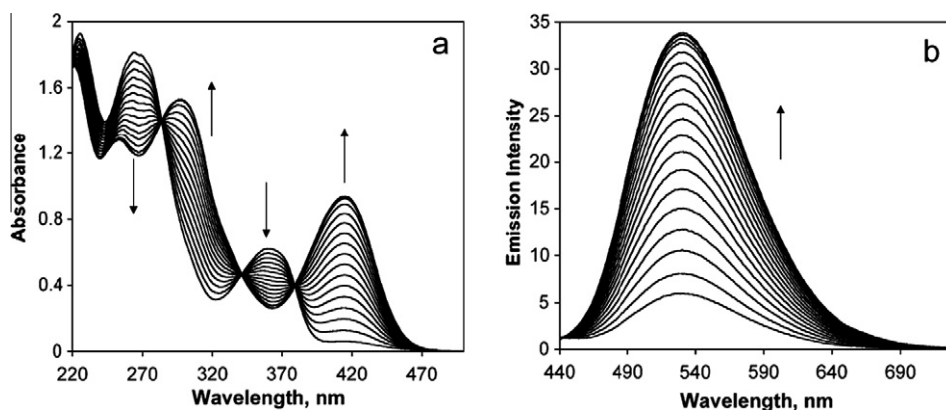


Fig. 12. Absorption (a) and emission (b) spectra of ligand **19** ($4.6 \times 10^{-5} \text{ M}$) in acetonitrile solutions upon the addition of $n\text{-Bu}_4\text{NF}$ [$(0\text{--}4.6) \times 10^{-5} \text{ M}$].

Table 4

Equilibrium constants for probes **19** and **20** in CH₃CN at 293 K as determined by absorption spectroscopic titrations.

Anion	Equilibrium constant K^a	
	Probe 19	Probe 20
F ⁻	$K_a = 2.5 \times 10^4$	$K_a = 3.1 \times 10^6$ $K_d = 1.1 \times 10^4$
CN ⁻	$K_a = 2.3 \times 10^5$	$K_{d1} = 6.4 \times 10^6$ $K_{d2} = 1.2 \times 10^6$
OAc ⁻	$K_a = 1.3 \times 10^5$	$K_{d1} = 1.4 \times 10^6$ $K_{d2} = 1.8 \times 10^3$
H ₂ PO ₄ ⁻	$K_a = 2.3 \times 10^3$	$K_a = 2.8 \times 10^4$
Cl ⁻	$K_a = 1.2 \times 10^2$	$K_a = 6.5 \times 10^3$
OH ⁻		$K_{d1} = 5.5 \times 10^6$ $K_{d2} = 2.6 \times 10^6$

^a The anions were added as tetrabutylammonium salts. K_a and K_d represent the association constants of anion–probe hydrogen-bonding complexes and proton dissociation constants of probe molecules, respectively.

ion resulted in significant luminescent quenching, with a quenching constant of $K_{sv} = 2.38 \times 10^4 \text{ M}^{-1}$, obtained from the Stern–Volmer plot. It required about 2 equiv. of Br⁻ to quench the emission

to 50% of the initial value, exhibiting a comparable level of sensitivity to anion as observed in the corresponding amide system [7].

In the absorbance spectrum of complex **13a**, the intensity of a band at ca. 230 nm was noted to increase when CN⁻ was added to the solution. Also observed was a slight bathochromic shift of approximately 10 nm, when up to 0.6 equiv. of TBA-CN was added. However, a lower energy band at 360 nm remained relatively unchanged both in position and intensity.

¹H NMR titrations studies of compounds **13a** and **16a** with fluoride anion, introduced as tetrabutylammonium fluoride (TBA-F) in CDCl₃, showed significant chemical shift changes of the thioamide and the thiourea (N–H) protons, respectively, upon addition of F⁻. This is indicative of strong hydrogen bonding interactions between the N–H groups and the anions.

Both anions showed significant quenching to the emission at low concentrations of 10^{-5} – 10^{-6} M (see Figs. 9 and 10). Additionally, **13b**-OTf was synthesized by known procedures and yielded the desired product which showed enhanced absorbance upon addition of TBA-H₂PO₄ in CH₂Cl₂ at 354 nm. The emission titration results were similar; therefore, the hexfluorophosphate counter ion could be interchangeably used with triflate.

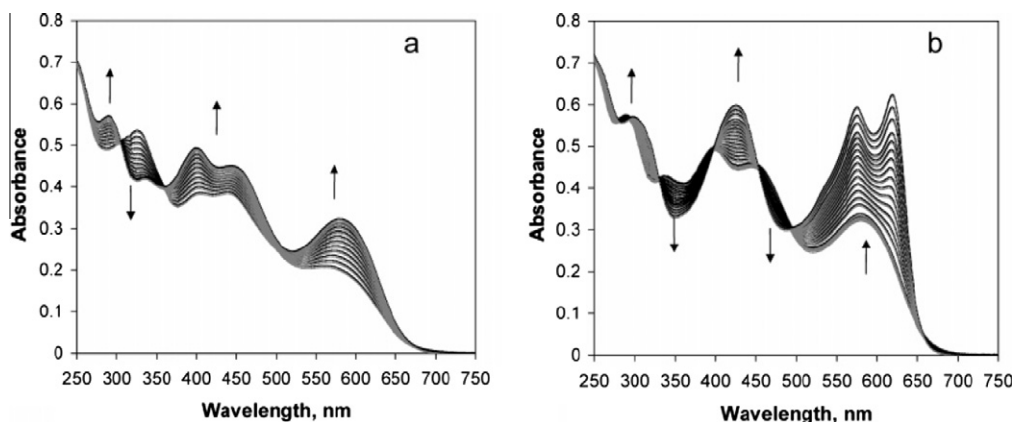


Fig. 13. Electronic absorption spectra of complex **20** (2.5×10^{-5} M) in CH₃CN upon the addition of *n*-Bu₄NF: (a) $[F^-] = (0\text{--}2.8) \times 10^{-5}$ M; (b) $[F^-] = 2.8 \times 10^{-5}$ – 1.1×10^{-4} M.

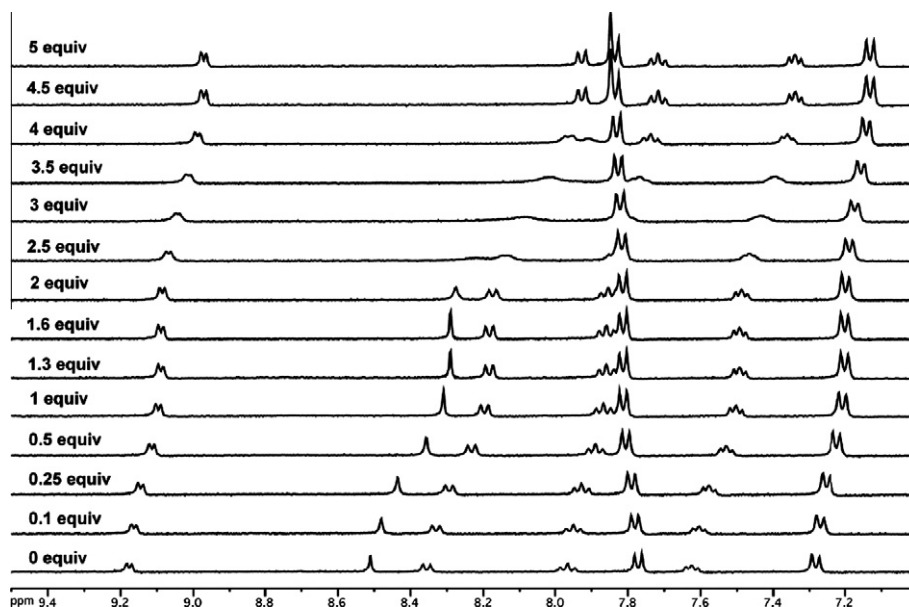


Fig. 14. ¹H NMR spectra of **20** in CD₃CN with the addition of *n*-Bu₄NF.

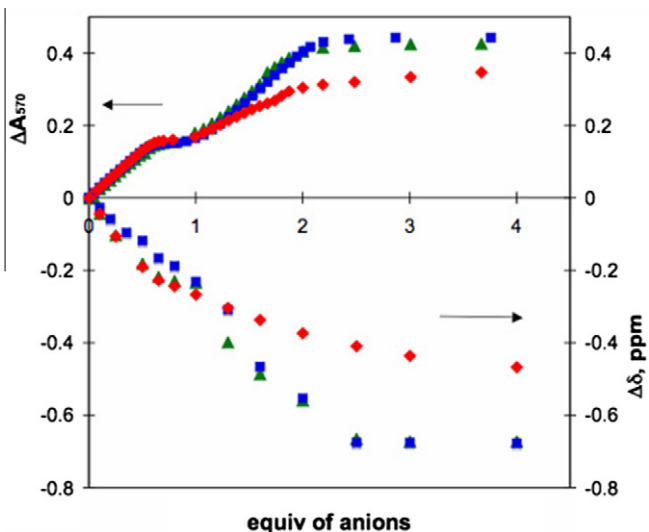


Fig. 15. Absorption (left, y axis) and ^1H NMR (right, y axis) spectral profiles of complex **20** with the addition of CN^- (green triangle curve), OAc^- (red diamond curve), and OH^- (blue square curve).

A modified complex based on the amidothiurea ligand **17**, was synthesized. This complex has the amidothiurea binding site located closer to the rhenium complex and the metal is bound para to the binding group. This is attached to a naphthyl group. Further observations indicate that this complex does have potential in cyanide anion recognition in an aqueous environment. Fig. 11 shows the results of emission quenching of compound **18** upon titration with CN^- in water. Other anions such as AcO^- , BzO^- , Br^- , Cl^- , H_2PO_4^- , F^- , I^- and ClO_4^- did not show any significant response.

4. Quinoxalinebis(sulfonamide) bridged rhenium(I) complex as a novel anion receptor

4.1. Preparation of quinoxalinebis(sulfonamide) bridged rhenium(I) complex

The syntheses of the sulfonamide ligand **19** and complex **20** are shown in Scheme 11. The bridging ligand **19** was synthesized from reaction of sulfonamide-functionalized diaminobenzene and the corresponding diketone in refluxing acetic acid in 95% yield. Subse-

quent reaction of **19** and $\text{BrRe}(\text{CO})_5$ in refluxing THF, followed by washing with THF and diethyl ether, afforded an orange-red powder of Re(I) complex **20**.

4.2. Photophysical properties

The absorption and emission spectral data along with lifetimes and emission quantum yields of ligand **19** and complex **20** are summarized in Table 3. Ligand **19** displays a series of absorption bands in the UV–Vis region, where the absorptions can be assigned to $\pi\text{--}\pi^*$ transitions. In contrast to the white color of ligand **19**, the Re(I) complex **20** is orange-red in the solid state. For complex **20** in CH_3CN , the absorption bands at 324 and 439 nm are assigned to ligand-centered $\pi\text{--}\pi^*$ transitions. The less intense absorption shoulder appearing at ca. 550 nm is assigned to a spin-allowed metal ($\text{Re}_d\pi$)-to-ligand (π^*) charge-transfer ($^1\text{MLCT}$) transition [17]. We envision that the incorporation of MLCT character in the probe molecules which is particularly sensitive to the surrounding micro-environment [18], a property that is essential for molecular recognition, would effectively promote the optical detecting limit and provide a more sensitive way to distinguish the incoming anionic substrates.

Ligand **19** shows a weak emission at 530 nm and a relatively short lifetime at 1.2 ns. The short lifetime of **19** suggests that the emission arises from a singlet $\pi\text{--}\pi^*$ excited state. Upon coordination to Re(I), the luminescence for complex **20** is only detectable in a deoxygenated solution with extremely low quantum yields, while the emission is completely quenched in an air-equilibrated solution. The luminescence of the rhenium(I) polypyridyl complex typically originates from the lowest $^3\text{MLCT}$ excited state because of the large spin orbital coupling exerted by Re(I), and the deactivation follows the energy gap law, where the nonradiative decay process becomes more efficient when the energy gap between the ground state and the emissive excited state is smaller because of greater vibrational overlap between the two electronic states [17]. Therefore, the luminescence decay for complex **20** is assigned to the $^3\text{MLCT}$ excited state and is anticipated to be dominated by a nonradiative process, with the fully π -conjugated structural framework of the ligand **19** effectively lowering the ligand π^* level, resulting in a smaller energy gap. The consequence here is the observation of the low luminescence quantum yield and short lifetime for complexes **20**, even in a deoxygenated solution.

4.3. Anion sensing studies

Fig. 12 illustrates absorption and emission titrations of ligand **19** upon the addition of F^- in a CH_3CN solution. In the electronic absorption spectrum, the tail at ~ 415 nm starts to grow accompanied with a decrease of the band at 355 nm and, concomitantly, the emission intensity at 530 nm shows an enhancement upon the addition of F^- ions. The appearance of a set of distinct isosbestic points indicates that the binding of F^- to ligand **19** is a clean equilibrium process. With reference to the spectroscopic studies of related sulfonamide compounds [19], it is likely that the observed changes in the absorption and emission spectra are a consequence of the hydrogen bonding of F^- to the sulfonamide N–H protons. Similar trends of spectral changes have been observed in absorption and emission spectra for ligand **19** upon the addition of OAc^- , CN^- , or H_2PO_4^- in a CH_3CN solution.

The UV–Vis absorption traces were further analyzed over the entire wavelength range using a nonlinear least-squares fit algorithm as implemented in the SPECFIT software package to extract the corresponding equilibrium constants. The obtained equilibrium constants are compiled in Table 4. In general, ligand **19** exhibits high sensitivity to CN^- , OAc^- , and F^- but, nevertheless, lacks good selectivity to explicitly differentiate these three anions.

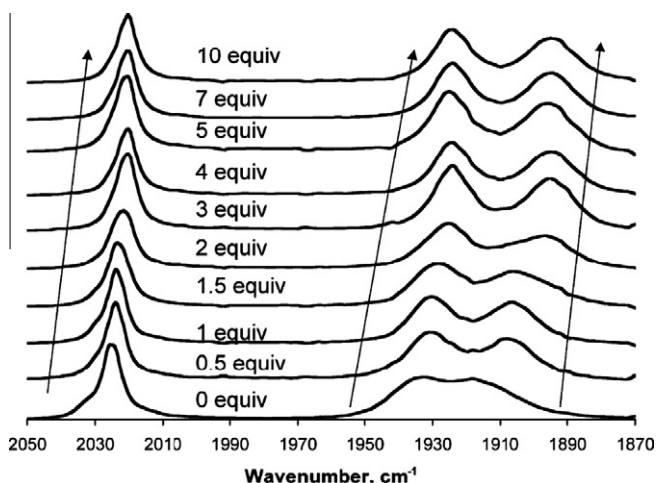


Fig. 16. Changes of $\nu(\text{CO})$ of complex **20** in the IR spectra upon the addition of $n\text{-Bu}_4\text{NF}$ in a CH_3CN solution.

The pK_a value of the sulfonamide N–H protons in ligand **19** is expected to become smaller upon coordination of Lewis acidic metal centers on the pyridylquinoxaline moiety of **19**. The overall effect is to effectively increase the sensitivity of the metal complex **20** to anions. In addition, the increasing acidity of the sulfonamide N–H protons also facilitates the tendency of complete proton transfer from probe molecule to basic anions.

Indeed, the addition of F^- to an acetonitrile solution of complex **20** resulted in an increase in the 1MLCT absorption band with sharp isosbestic points at 305 and 354 nm (see Fig. 13a), indicating a clean well-defined equilibrium in solution. After more than 1 equiv. of F^- was added, however, the 1MLCT absorption band was further intensified and red-shifted, with a new set of isosbestic points appearing at 287, 330, 396, 452, and 492 nm (see Fig. 13b). Similar two-step equilibrium phenomena were also observed in the titration of CN^- or OAc^- to the solution of complex **20**. Job plots confirm the 1:2 stoichiometry between complex **20** and these anions. However, only a single equilibrium was observed in the UV–Vis absorption response similar to the profile shown in Fig. 13a upon the addition of $H_2PO_4^-$ or Cl^- ions, and the job plots show a 1:1 stoichiometry for both anions.

The stepwise process observed in the spectrophotometric titration with F^- can be described by two stepwise equilibria: (1) formation of a hydrogen-bound complex via sulfonamide N–H protons with an incoming anion followed by (2) deprotonation of the acidic sulfonamide N–H proton to form mono-deprotonated complex **20** and HF_2^- . Fig. 14 displays the 1H NMR titration spectra of complex **20** with $n-Bu_4NF$, and a hydrogen-bond-induced upfield shift was observed in the singlet signal of quinoxaline upon the addition of a first 1 equiv. of F^- in a CD_3CN solution of complex **20**. The proton signals hardly move between additions of 1 and 2 equiv. of F^- . Subsequently, further upfield shifts of the proton signals are observed again with the amount of added F^- over 2 equiv.

In the cases of CN^- and OAc^- , the spectrophotometric responses are attributed to a stepwise double deprotonation. Complex **20** was further titrated by $n-Bu_4NOH$ to confirm that the double deprotonation indeed occurred during the course of CN^- and OAc^- titrations. The very similar titration isotherms of the absorption band at 570 nm as well as the upfield shift of the quinoxaline proton signals upon the addition of OH^- , CN^- , and OAc^- are shown in Fig. 15. These results suggest that complex **20** undergoes a stepwise double proton transfer in the presence of CN^- or OAc^- . The less basic $H_2PO_4^-$ and Cl^- ions show no ability to deprotonate the sulfonamide N–H protons, where the proton signals upfield shift and reach the maximum shift at the 1 equiv. addition of $H_2PO_4^-$ (see Fig. 16) and, thus, form only simple 1:1 hydrogen bonding complexes with complex **20**.

The stretching frequencies of the metal carbonyl in complex **20** provide an additional channel to probe the remote probe–anion interactions [20]. The typical CO stretching frequencies of metal carbonyl complexes appear at 1700 – 2100 cm^{-1} , a region that is usually free of other ligand vibrations. With the $Re(I)$ site symmetry of C_s , the IR $\nu(CO)$ bands of complex **20** are typical of three CO stretches: two of A' symmetry and one of A'' symmetry [21]. The extent of $Re(I)$ π back-bonding to the metal carbonyl would be directly correlated to the electron density on the chelating dipyritylquinoxaline ligand. In other words, one would expect that the higher electron density on the chelating ligand would result in a stronger π back-bonding to the $Re(I)$ –C bond and, thus, reduce the IR stretching frequencies of the metal carbonyl.

On the basis of the results obtained from 1H NMR and UV–Vis spectrophotometric titration experiments, the electron density of the chelating dipyritylquinoxaline ligand is expected to increase with the formation of a hydrogen bond and/or deprotonation of the sulfonamide N–H by the incoming anions. Indeed, the IR $\nu(CO)$

bands of complex **20** shift to lower frequencies upon anion addition. Fig. 16 illustrates the shift of the IR $\nu(CO)$ bands of complex **20** upon the addition of F^- in a CH_3CN solution. The shift of the carbonyl group frequency is in the order of $CN^- > F^- \approx OAc^- > H_2PO_4^- > Cl^-$, which is consistent with the results obtained from 1H NMR and UV–Vis spectrophotometric titrations.

5. Concluding remarks

We have demonstrated in this review that different types of rhenium(I) carbonyls complexes with polarized N–H recognition motifs can be designed and synthesized as anion receptors. In particular, the selectivity for different anions is greatly enhanced upon coordination of organic probe to transition metals. The incorporation of potential luminescent chromophores into the structure provides a very sensitive way to detect the presence of the anions. The degrees of probe–anion interactions can be easily visualized via naked eye colorimetric or luminescent responses.

Acknowledgments

We are grateful to the Division of Chemical Sciences, Office of Basic Energy Sciences, Office of Energy Research, US Department of Energy for support of the research carried out at State University of New York at Binghamton and the National Science Council of Taiwan for support of the research carried out at Academia Sinica. Dr. K.-C. Chang thanks the postdoctorate fellowship sponsored by Academia Sinica.

References

- [1] R. Martínez-Mañez, F. Sancenón, *Chem. Rev.* 103 (2003) 4419. and references therein.
- [2] P.D. Beer, P.A. Gale, *Angew. Chem., Int. Ed.* 40 (2001) 486.
- [3] [a] Y. Marcus, *J. Chem. Soc., Faraday Trans. 1* (87) (1991) 2995; [b] Y. Marcus, *J. Chem. Soc., Faraday Trans. 1* (83) (1987) 339; [c] Y. Marcus, *J. Chem. Soc., Faraday Trans. 1* (82) (1986) 233.
- [4] A. Bianchi, K. Bowman-James, E. García-España (Eds.), *Supramolecular Chemistry of Anions*, Wiley-VCH Publishers, Toronto, Canada, 1997.
- [5] (a) A.P. De Silva, H.Q. Gunaratne, N.T. Gunnlaugsson, A.J.M. Huxley, C.P. McCoy, J.T. Rademacher, T.E. Rice, *Chem. Rev.* 97 (1997) 1515; (b) M.H. Keefe, K.D. Benkstein, J.T. Hupp, *Coord. Chem. Rev.* 205 (2000) 201; (c) C.-Y. Wu, M.-S. Chen, C.-A. Lin, S.-C. Lin, S.-S. Sun, *Chem. Eur. J.* 12 (2006) 2263; (d) C.-L. Chen, Y.-S. Chen, C.-Y. Chen, S.-S. Sun, *Org. Lett.* 8 (2006) 5053; (e) C.-L. Chen, T.-P. Lin, Y.-S. Chen, S.-S. Sun, *Eur. J. Org. Chem.* (2007) 3999; (f) C.-Y. Chen, T.-P. Lin, C.-K. Chen, S.-C. Lin, M.-C. Tseng, Y.-S. Wen, S.-S. Sun, *J. Org. Chem.* 73 (2008) 900; (g) Z. Lin, H.-C. Chen, S.-S. Sun, C.-P. Hsu, T.J. Chow, *Tetrahedron* 65 (2009) 5216; (h) A.S. Singh, S.-S. Sun, *Chem. Commun.* 47 (2011) 8563.
- [6] Recent examples on transition-metal based luminescence sensing systems: (a) L.J. Charbonnière, R. Ziessel, M. Montalti, L. Prodi, N. Zaccheroni, C. Boehme, G. Wipff, *J. Am. Chem. Soc.* 124 (2002) 7779; (b) P. Anzenbacher Jr., D.S. Tyson, K. Jursíková, Castellano; (c) S.-S. Sun, J.A. Anspach, A.J. Lees, P.Y. Zavalij, *Organometallic* 21 (2002) 685; (d) C.-Y. Hung, A.S. Singh, C.-W. Chen, Y.-S. Wen, S.-S. Sun, *Chem. Commun.* (2009) 1511; (e) B.-C. Tzeng, Y.-F. Chen, C.-C. Wu, C.-C. Hu, Y.-T. Chang, C.-K. Chen, *New J. Chem.* 31 (2007) 202; (f) Z.-H. Lin, S.-J. Ou, C.-Y. Duan, B.-G. Zhang, Z.-P. Bai, *Chem. Commun.* (2006) 624; (g) A. Kumar, S.-S. Sun, A.J. Lees, *Coord. Chem. Rev.* 252 (2008) 922; (h) A. Kumar, S.-S. Sun, A.J. Lees, *Top. Organomet. Chem.* 29 (2010) 1; (i) A.S. Singh, S.-S. Sun, *J. Org. Chem.* 77 (2012) 1880.
- [7] (a) S.-S. Sun, A.J. Lees, *Chem. Commun.* (2000) 1687; (b) S.-S. Sun, A.J. Lees, P.Y. Zavalij, *Inorg. Chem.* 42 (2003) 3445.
- [8] S.-S. Sun, A.J. Lees, *Coord. Chem. Rev.* 230 (2002) 171.
- [9] (a) M.O. Odago, A.E. Hoffman, R.L. Carpenter, D.C.T. Tse, S.-S. Sun, A.J. Lees, *Inorg. Chim. Acta* 374 (2011) 558; (b) M.O. Odago, D.M. Colabello, A.J. Lees, *Tetrahedron* 66 (2010) 7465.
- [10] T.-P. Lin, C.-Y. Chen, Y.-S. Wen, S.-S. Sun, *Inorg. Chem.* 46 (2007) 9201.
- [11] (a) A.P. Bisson, V.M. Lynch, M.-K.C. Monahan, E.V. Anslyn, *Angew. Chem., Int. Ed. Engl.* 36 (1997) 2340; (b) C.A. Hunter, L.D. Sarson, *Angew. Chem., Int. Ed. Engl.* 33 (1994) 2313; (c) K.-S. Jeong, Y.L. Cho, J.U. Song, H.-Y. Chang, M.-G. Choi, *J. Am. Chem. Soc.*

- 120 (1998) 10982;
(d) C.A. Hunter, C.M.R. Low, M.J. Packer, S.E. Spey, J.G. Vinter, M.O. Vysotsky, C. Zonta, *Angew. Chem., Int. Ed.* 40 (2001) 2678;
(e) B. Huang, J.R. Parquette, *Org. Lett.* 2 (2000) 239;
(f) Y. Hamuro, S.J. Geib, A.D. Hamilton, *Angew. Chem., Int. Ed. Engl.* 33 (1994) 446.
- [12] (a) A.I. Baba, J.R. Shaw, J.A. Simon, R.P. Thummel, R.H. Schmehl, *Coord. Chem. Rev.* 171 (1998) 43;
(b) S.-S. Sun, E. Robson, N. Dunwoody, A.S. Silva, I.M. Brinn, A.J. Lees, *Chem. Commun.* (2000) 201;
(c) J.-L. Lin, C.-W. Chen, S.-S. Sun, A.J. Lees, *Chem. Commun.* 47 (2011) 6030.
- [13] I. Chao, T.-S. Hwang, *Angew. Chem., Int. Ed.* 40 (2001) 2775.
- [14] K.A. Connors, *Binding Constant*, Wiley, New York, 1987.
- [15] C.G. Coates, T.E. Keyes, J.J. McGarvey, H.P. Hughes, J.G. Vos, P.M. Jayaweera, *Coord. Chem. Rev.* 171 (1998) 323.
- [16] (a) T.S. Snowden, A.P. Bisson, E.V. Anslyn, *J. Am. Chem. Soc.* 121 (1999) 6324;
(b) K. Kavallieratos, S.R. de Gala, D.J. Austin, R.H. Crabtree, *J. Am. Chem. Soc.* 119 (1997) 2325.
- [17] (a) P.H. Dinofu, V. Coropceanu, J.-L. Brédas, J.T. Hupp, *J. Am. Chem. Soc.* 128 (2006) 12592;
(b) K.A. Walters, K.D. Ley, C.S.P. Cavalheiro, S.E. Miller, D. Gosztola, M.R. Wasielewski, A.P. Bussandri, H. van Willigen, K.S. Schanze, *J. Am. Chem. Soc.* 123 (2001) 8329;
(c) S.-S. Sun, A.J. Lees, *J. Am. Chem. Soc.* 122 (2000) 8956;
(d) A.I. Baba, J.R. Shaw, J.A. Simon, R.P. Thymmel, R.H. Schmehl, *Coord. Chem. Rev.* 171 (1998) 43;
(e) H.D. Stoeffler, N.B. Thornton, S.L. Temkin, K.S. Schanze, *J. Am. Chem. Soc.* 117 (1995) 7119;
(f) J.A. Baiano, R.J. Kessler, R.S. Lumpkin, M.J. Munley, W.R. Murphy Jr., *J. Phys. Chem.* 99 (1995) 17680;
(g) L.A. Worl, R. Duesing, P. Chen, L.D. Ciana, T.J. Meyer, *J. Chem. Soc., Dalton Trans.* (1991) 849;
(h) A.J. Caspar, T.J. Meyer, *J. Phys. Chem.* 87 (1983) 952.
- [18] A.J. Lees, *Comments Inorg. Chem.* 17 (1995) 319.
- [19] (a) Y. Wu, X. Peng, J. Fan, S. Gao, M. Tian, J. Zhao, S. Sun, *Org. J. Chem.* 72 (2007) 62;
(b) S.D. Starnes, S. Arungundram, C.H. Saunders, *Tetrahedron Lett.* 43 (2002) 7785.
- [20] (a) L. Ion, D. Morales, S. Nieto, J. Pérez, L. Riera, D. Miguel, R.A. Kowenick, M. McPartlin, *Inorg. Chem.* 46 (2007) 2846;
(b) E. Peris, J.A. Mata, V. Moliner, *J. Chem. Soc., Dalton Trans.* (1999) 3893.
- [21] R.H. Crabtree, *The Organometallic Chemistry of the Transition Metals*, third ed., Wiley, New York, 2001.